Parameter allocation of parallel array bistable stochastic resonance and its application in communication systems*

Jian Liu(刘健)[1], You-Guo Wang(王友国)[2,3,†], Qi-Qing Zhai(翟其清)[1], and Jin Liu(刘进)[4]

[1] College of Communication and Information Engineering, Nanjing University of Posts and Telecommunications, Nanjing 210003, China
[2] College of Science, Nanjing University of Posts and Telecommunications, Nanjing 210023, China
[3] Jiangsu Innovative Coordination Center of Internet of Things, Nanjing University of Posts and Telecommunications, Nanjing 210003, China
[4] 20th Research Institute of China Electronics Technology Corporation, Xi'an 710068, China

(Received 29 January 2016; revised manuscript received 29 May 2016; published online 25 August 2016)

In this paper, we propose a parameter allocation scheme in a parallel array bistable stochastic resonance-based communication system (P-BSR-CS) to improve the performance of weak binary pulse amplitude modulated (BPAM) signal transmissions. The optimal parameter allocation policy of the P-BSR-CS is provided to minimize the bit error rate (BER) and maximize the channel capacity (CC) under the adiabatic approximation condition. On this basis, we further derive the best parameter selection theorem in realistic communication scenarios via variable transformation. Specifically, the P-BSR structure design not only brings the robustness of parameter selection optimization, where the optimal parameter pair is not fixed but variable in quite a wide range, but also produces outstanding system performance. Theoretical analysis and simulation results indicate that in the P-BSR-CS the proposed parameter allocation scheme yields considerable performance improvement, particularly in very low signal-to-noise ratio (SNR) environments.

Keywords: stochastic resonance, parameter allocation, bit error rate, channel capacity

PACS: 05.40.–a, 02.50.–r, 43.60.Dh **DOI:** 10.1088/1674-1056/25/10/100501

1. Introduction

Noise can sometimes enhance the responses of certain nonlinear systems. This counterintuitive phenomenon is termed as stochastic resonance (SR), which dates back to meteorology for its original discovery[1] and develops to a wide variety of fields.[2–36] The SR method employs the appropriately added noise to yield superior system response using various measures, such as signal-to-noise ratio (SNR) gain,[7] Fisher information,[8] correlation coefficient,[9] and stimulus-specific information.[10]

Threshold systems (TSs) are often used in exhibiting the SR effect.[6,8–14] Chen *et al.* proved that optimal additive noise is a randomization of two discrete signals in sign detectors.[12] Guo *et al.* designed the optimal binary threshold detector that maximizes the area under the ROC curve.[13] In Ref. [6], we have proposed a single TS-based detector to achieve preferable binary hypothesis-testing performance by considering both additive Gaussian background noise and four representative multiplicative external noises. However, the implementation of SR via adding additional noise is inappropriate for "over-resonant", where the background noise exceeds the resonance region.

To overcome the aforementioned restrictions in TSs, Xu *et al.*[15] employed the dynamic bistable system to propose the parameter-induced SR theory, which extends the conventional SR theory[16] to communication application. Based on the extended SR theory, several parameter allocation approaches in bistable SR (BSR) models for weak signal processing have been studied.[17–20] Yang *et al.*[17] adjusted the parameter of a BSR system to achieve the high bit rates of the logical signals. Wang *et al.*[18] introduced the BSR into a cognitive radio system to improve spectrum sensing performance. Recently, we quantitatively investigated the parameter selection of the BSR system for transmitting BPSK and BPAM signals, and showed a significant improvement of BER performance and SNR wall.[19,20] But for the previous works,[19,20] these schemes failed to make full use of the SR effect. First, the parameter allocation of the BSR system in the framework of adiabatic approximation only guarantees the occurrence of SR, and cannot reach the best SR effect. Meanwhile, a reliable and stable communication performance is not sustainable under very low SNR environments. Thus, an optimal and robust parameter-induced SR strategy is worthy of attention in extremely noisy communication scenarios. In a parallel summing network, the overall output can yield a net gain in information from all SR subsystems.[21] Moreover, Duan *et al.*[22,23] formulated the array SR theory in an uncoupled parallel array of the BSR (P-BSR) system and derived the SNR gain can be greater than one. Unlike uncoupled dynamic systems, Kang *et al.*[24] adopted two linearly interacting overdamped bistable oscillators to explore the effect of spatially correlated

*Project supported by the National Natural Science Foundation of China (Grant No. 61179027), the Qinglan Project of Jiangsu Province of China (Grant No. QL06212006), and the University Postgraduate Research and Innovation Project of Jiangsu Province (Grant Nos. KYLX15_0829, KYLX15_0831).

†Corresponding author. E-mail: wyg@njupt.edu.cn

© 2016 Chinese Physical Society and IOP Publishing Ltd

noise on the SR phenomenon. So far, the idea of an "array-aided effect" has been considered in ensembles of coupled SR systems,[24–29] threshold comparators,[14,30–32] and dynamic bistable oscillators.[33–35]

To investigate both the optimal and robust parameter allocation policy and the array-aided effect, in this paper, we explore a P-BSR-based communication system (P-BSR-CS) to transmit BPAM signals under very low SNR. First, in the adiabatic approximation framework, the parameter allocation range of the P-BSR-CS is deduced and the optimal parameter combination is searched from the SR-operative range to establish an optimal referential BSR model. We find that, with the numbers of array elements increasing, the optimal parameter pair is not fixed but variable in quite a wide range. Second, aimed at the maximum bit error rate (BER) reduction and channel capacity (CC) improvement in realistic communication scenarios, a parameter allocation theorem concerning the P-BSR-CS for performance improvement is derived. Third, the proposed parameter allocation scheme can adaptively adjust the parameter of the P-BSR for different SNRs. Our policy guarantees both the maximum use of the SR effect and the robustness of parameter selection optimization. The simulation results show that in the P-BSR the proposed parameter allocation scheme can significantly yield superior performance, which verifies the theoretical analysis.

The rest of the paper is arranged as follows. In Section 2, a P-BSR-CS model is presented. In adiabatic approximation framework, an optimal parameter allocation policy of the P-BSR-CS for BPAM signal transmissions is given in Section 3, followed by its extension to realistic communication scenarios in Section 4. Theoretical analysis and simulation results are discussed in Section 5. Finally, Section 6 concludes the paper.

2. A P-BSR-CS model

The schematic diagram of the proposed P-BSR-CS is described in Fig. 1. In this model, the P-BSR-CS consists of five basic elements, namely, binary signal sequence S_i $(i=1,2,\ldots,+\infty)$, transmitter, multipath channels with the addition of nonlinear BSR subsystems, receiver, and recovered binary signal Y_i. At the transmitter, symbol information is modulated by periodic rectangular pulse; afterwards, the BPAM signal propagates through multipath additive white Gaussian noise (AWGN) channels and array bistable systems, which have outputs as $r_j(t)$ and $x_j(t)$ $(j=1,2,\ldots,L)$ respectively, the received signal carrying symbol information from the L-th bistable systems can be written as $y(t)=1/L\sum_{j=1}^{L}x_j(t)$, then the received signal turns into the recovered binary signal after detection and decision. In order to primarily explore the array-aided SR effect, our channels are the simplified version of the actual multipath channels. The j-th bistable device corresponding to the j-th multipath channel is subject to independent identically distributed (*i.i.d.*) AWGN $\xi_j(t)$ with autocorrelation $\langle\xi_j(t)\xi_j(t+\tau)\rangle=\sigma_\xi^2\delta(\tau)$, where $\delta(\cdot)$ denotes the Dirac function.

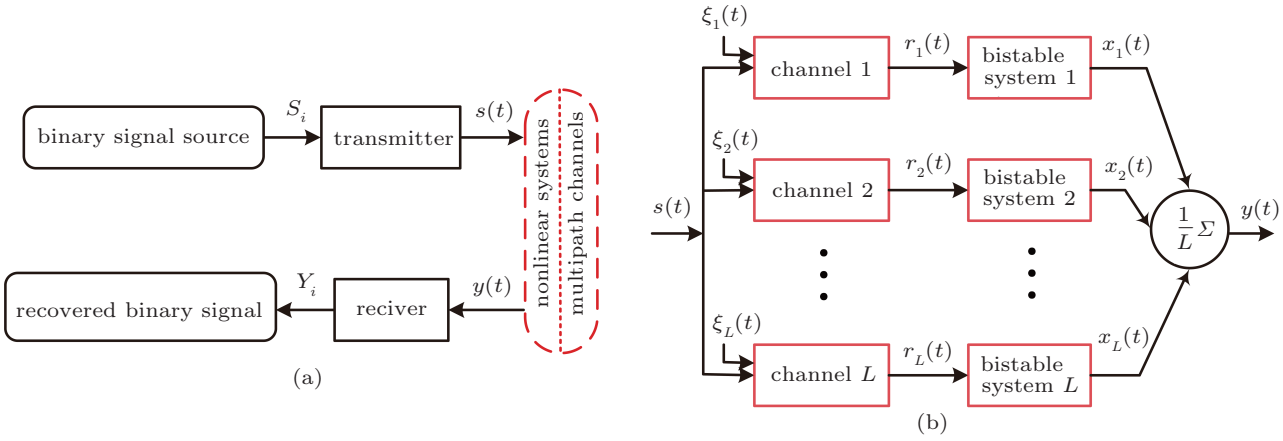


Fig. 1. (color online) (a) A P-BSR-CS model. (b) Structure of multipath AWGN channels and parallel bistable nonlinear systems acting as the red dashed line part in the P-BSR-CS.

Through the above description, the signal transmission problem in the P-BSR-CS model can be deemed to be a decision problem of a binary hypothesis testing as follows:

$$\begin{aligned}\mathscr{H}_1&:\ \text{transmit symbol}\quad 1,\\ \mathscr{H}_0&:\ \text{transmit symbol}\ -1.\end{aligned}\tag{1}$$

A BPAM signal $s(t)$ is associated with information symbol sequence S_i, which carries useful information with the following shape

$$s(t)=A\sum_{i=1}^{+\infty}S_iG(t-\mathrm{i}T),\tag{2}$$

where A denotes an amplitude of signal $s(t)$, S_i represents the signal symbols sequence of the BPAM signal, which can be taken from the binary set $\{1,-1\}$, and $G(t)$ is a rectangular pulse of duration T, which can be expressed as

$$G(t)=\begin{cases}1, & \text{if } t\in(0,T),\\ 0, & \text{else.}\end{cases}\tag{3}$$

From Eqs. (1), (2), and (3), we also have the following probabilities relationship

$$\begin{cases} P(S_i = 1) = P(s(t) = A), & \text{under } \mathscr{H}_1, \\ P(S_i = -1) = P(s(t) = -A), & \text{under } \mathscr{H}_0. \end{cases} \tag{4}$$

In this research, we adopt a group of nonlinear dynamical BSR subsystems to demonstrate the array-aided effect, which receives inspiration from the array SR theory[23] (the SNR gain can be further improved by array SR, particularly in the case of strong noise whose intensity exceeds the conventional SR region). Subsequently, the P-BSR scheme is modeled by jointly considering these nonlinear BSR subsystems, given as

$$\frac{\mathrm{d}\boldsymbol{x}}{\mathrm{d}t} = a\boldsymbol{x} + \mu\boldsymbol{x} + s(t) + \boldsymbol{\xi}, \tag{5}$$

where

$$\boldsymbol{x} = [x_1(t), x_2(t), \ldots, x_L(t)]^{\mathrm{T}},$$
$$\boldsymbol{\xi} = [\xi_1(t), \xi_2(t), \ldots, \xi_L(t)]^{\mathrm{T}}.$$

Obviously, an optimal P-BSR system is equivalent to optimal BSR subsystems due to the parallel array processing architecture. Without loss of generality, we merely consider a Brownian particle hopping in a double-well potential subject to AWGN as the BSR subsystem, and obtain the Langevin equation[16]

$$\begin{cases} \dfrac{\mathrm{d}x_j}{\mathrm{d}t} = -\dfrac{\partial U_j(x_j,t)}{\partial x_j} + \xi_j(t), \\ U_j(x_j,t) = -\dfrac{a}{2}x_j^2 + \dfrac{\mu}{4}x_j^4 - s(t)x_j, \end{cases} \tag{6}$$

where a ($a > 0$) and μ ($\mu > 0$) are the parameters of the BSR system, $U_j(x_j,t)$ denotes the quartic potential function in the presence of a modulating signal $s(t)$, which can be interpreted as the motion trail of the BSR system output x_j. As a rule, we can employ the fourth-order Runge–Kutta algorithm to numerically solve the differential equation (6), to be specific, set $u' = g(t,u)$, the fourth Runge–Kutta numerical algorithm can be operated by

$$u_{n+1} = u_n + (h/6)(k_1 + 2k_2 + 3k_3 + k_4),$$

where $k_1 = g_n$, $k_2 = g(t_n + h/2, u_n + (h/2)k_1)$, $k_3 = g(t_n + h/2, u_n + (h/2)k_2)$, $k_4 = g(t_{n+1}, u_n + hk_3)$, and h is the step size.

In Fig. 2(a), the quartic potential has two stable states (potential well) at $x_j = \pm c = \pm\sqrt{a/\mu}$ and $\Delta U_j = a^2/4\mu$ denotes the barrier height. Hence, the height of the potential barrier and the location of the potential well can be controlled by modulating parameters a and μ. The output signal $x_j(t)$ lies on the location of the stable state $x_j = \pm c$ in defect of signal and noise force driving. Throughout this paper, we assume that the BPAM signal amplitude is small enough ($A < A_{c0}$), where $A_{c0} = \sqrt{4a^3/27\mu}$ stands for the static threshold of the bistable system.[16] Therefore, only the presence of signal forcing is a lack of enough energy to trigger the output response transitions between the two potential wells, as shown in Fig. 2(b).

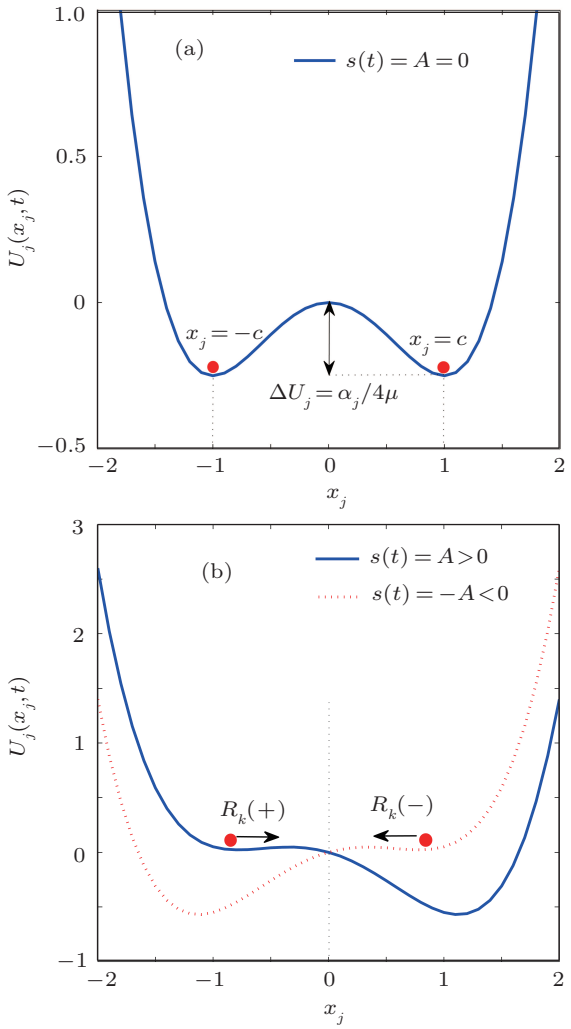


Fig. 2. (color online) $a = 1$, $\mu = 1$, $\xi_j(t) = 0$ (a) the quartic potential function $U_j(x_j,t)$ driven by no signal forcing ($s(t) = 0$); (b) the quartic potential function $U_j(x_j,t)$ driven by signal forcing at two symmetric amplitudes ($s(t) = A = 0.3$ or $s(t) = -A = -0.3$).

The modulated amplitude of the BPAM signal has the effect of adjusting the transition rate, making $R_k(\pm)$, the rate from the $\mp$ well to the $\pm$ well when the input signal switches from the amplitude $\mp A$ to $\pm A$. Yet if the noise force driving is very small, these rates are still too slow so that the output response does not have enough energy to hop over the barrier. As the increasing variance of the input noise σ_ξ^2, the rate at which such jumps will occur, $R_k(+)$ and $R_k(-)$, increases. Due to the symmetric structure in a quartic potential function of the bistable system, we get $R_k(+) = R_k(-) = R_k$. However, since the bistable system is subjected to both a signal forcing and a moderate amount of random noise forcing, there is a cooperation of BPAM signal, noise and quartic potential taking place: one part of the in-coherent noise energy transfers into the coherent output signal, then the input signal receives

assistance from noise to trigger a stronger response from the nonlinear bistable system.

According to Ref. [20], we employ an analogous decoding method to enable restoration of the input binary BPAM signals accurately. Herein, we assume that the input information-bearing symbols S_i are transmitted at the rate of one symbol per a duration T, since then, each new symbol starts at $t = iT$ and sustains over a duration of T. The key of our detection mechanism is that one can continuously recover the input BPAM symbols $S_i = \pm 1$ from the observation of the system output response $y(t)$. It is demanded that at the decoding time $t = t_i + T$ the Brownian particle has already arrived at the vicinity of the stable state

$$x_j = \sqrt{a/\mu} \quad \left(\text{or } x_j = -\sqrt{a/\mu}\right)$$

corresponding to the input BPAM signal amplitude changes in switching from $-A$ to A (or inversely). Consequently, the decoding process of the receiver in the P-BSR-CS can be given as

$$Y_i = \begin{cases} 1, & y(t_i + T) > 0, \\ -1, & y(t_i + T) < 0. \end{cases} \tag{7}$$

For the P-BSR-CS, the probability of error bits $P(1|-1)$ takes place in that when the input signal amplitude is $-A$ the system output response locates below the decision threshold; similarly, $P(-1|1)$ denotes that when the input signal is A the system output response is greater than the decision threshold. Consequently, the BER of the P-BSR-CS is the sum of probability of error bits, which is used as a quantitative performance metric, can be expressed as

$$P_{\mathrm{e}} = P(-1)P(1|-1) + P(1)P(-1|1). \tag{8}$$

Alternatively, channel capacity (CC) is the tight upper bound rate of transmitting reliable information over a system, which can be regarded as another metric.[36] Using Eq. (8), the CC of the P-BSR-CS (C) can be written as the function of BER (P_{e})

$$C = R_{\mathrm{b}}[1 + P_{\mathrm{e}}\log_2 P_{\mathrm{e}} + (1 - P_{\mathrm{e}})\log_2(1 - P_{\mathrm{e}})], \tag{9}$$

where R_{b} represents the bit rate of the input signal symbol and it can be expressed as the reciprocal of the symbol interval T ($R_{\mathrm{b}} = 1/T$).

3. Parameter allocation policy under the adiabatic approximation condition

According to adiabatic approximation theorem[16] and parameter-induced SR theorem,[15] we declare that the optimal P-BSR-CS can be implemented by modulating the system parameters a and μ, respectively. Xu *et al.*[15] introduced the notion of system response time T_{response} to depict the time where the Brownian particle switches from one potential well to the other driven by $r_j(t) = s(t) + \xi_j(t)$ in the bistable system. The key idea of realizing SR is to guarantee that the system response time T_{response} and the symbol interval T should satisfy the following inequality

$$T_{\mathrm{response}} < T. \tag{10}$$

Consider the adiabatic approximation condition ($A \ll 1$, $T \gg 1$, $\sigma_\xi^2 \ll 1$) and the absence of input BPAM signal, the physical meaning of the Kramer rate is the rate of the output of BSR subsystems hopping from one potential well to the other

$$R_{\mathrm{k}} = \frac{a}{\sqrt{2}\pi}\exp\left(-\frac{2\Delta U_j}{\sigma_\xi^2}\right) = \frac{a}{\sqrt{2}\pi}\exp\left(-\frac{a^2}{2\mu\sigma_\xi^2}\right). \tag{11}$$

From the above analyses, the response time T_{response} is driven by both the signal and the noise while the Kramer rate R_{k} is only driven by the noise. Thus, we have the following inequality as

$$\frac{1}{R_{\mathrm{k}}} > T_{\mathrm{response}}. \tag{12}$$

Combined with the formulas (10), (11), and (12), it yields that

$$\frac{1}{R_{\mathrm{k}}} \leq T. \tag{13}$$

Furthermore, according to the classical BSR theory, the output signal of the BSR system is enhanced optimally when the noise variance equals to half of the barrier height ($\sigma_\xi^2 = \Delta U_j/2$).[16–20]

Hence, we can obtain the parameter allocation when SR works after performing straightforward calculation. For the information-bearing BPAM input signal, the SR-operative parameter selection of the P-BSR system is given as

$$\begin{cases} a = a_{(\mathrm{SR})} \geq \sqrt{2}\pi e(1/T_{\mathrm{SR}}), \\ \mu = \mu_{(\mathrm{SR})} = a_{(\mathrm{SR})}^2/(2\sigma_{\xi_{\mathrm{SR}}}^2), \end{cases} \tag{14}$$

where symbol interval $T = T_{\mathrm{SR}}$ and noise variance $\sigma_\xi^2 = \sigma_{\xi_{\mathrm{SR}}}^2$ pertain to the adiabatic approximation category.[16]

Remark 1 From the above analyses, we can see that the optimal SR effect of the BSR subsystem can be determined by the parameter allocation optimization $\left(a = a_{(\mathrm{SR})}^{\mathrm{opt}}, \mu = \mu_{(\mathrm{SR})}^{\mathrm{opt}}\right)$ and μ is completely decided by a. Crucially, it provides the potential theoretical basis to the proposed P-BSR-CS.

Remark 2 What is the range of a? Actually, a is only a relative large value, moreover, too small or too large cannot reach the SR-operative region. Our goal is to find out optimal a from the SR-operative parameter scope $a_{(\mathrm{SR})}$ to form $a_{(\mathrm{SR})}^{\mathrm{opt}}$ using the search method, as shown in Fig. 3.

Remark 3 It is noticeable now that if the characteristic of BPAM input signal and AWGNs cannot satisfy the adiabatic approximation condition, the SR phenomenon will not happen. This point will be dealt with in detail in the next section. Therefore, the parameter allocation policy of the P-BSR-CS only works in the adiabatic approximation regime like symbol interval T_{SR} and noise variance $\sigma_{\xi_{\mathrm{SR}}}^2$ at this moment.

Figure 3 displays the BER of the optimal linear detection and the P-BSR-CS in different array numbers. Our parameter allocation scheme aims at minimizing the BER at the signal receiver by selecting the appropriate system parameter. From the view of perception, the yellow area under the red curve and over the blue curve represents the SR-operative region. Compare the four subfigures, the SR-operative region extends with the increasing of the array number and the scope of optimal parameter a, which enables the BER to approach 0, enlarges in its neighborhood. It can also be seen that the detection performance of the P-BSR-CS with exceedingly small parameter $(a \to 0)$ keeps in bad operating and is inferior to that of traditional optimal linear detection without nonlinear SR structure in large parameter regions. Once we chose a relatively large a, in the case of the array scheme, it can still satisfy the detection performance because of the wide region of parameter a. The uncertainty of noise can also lead to an incorrect parameter selection, which results in operating SR technology improperly. Fortunately, we can overcome this shortcoming by adaptively choosing the system parameter to obtain the minimal BER, which mitigates the influence of noise uncertainty. Therefore, the ideal parameter selection in Refs. [19] and [20] $(1,1)$ is only a special one (not the optimal combination) of the SR-operative region from the perspective of recovery-correct output waveform. So, we provide an optimal parameter allocation policy and an array-aided idea to maximize the use of the SR effect.

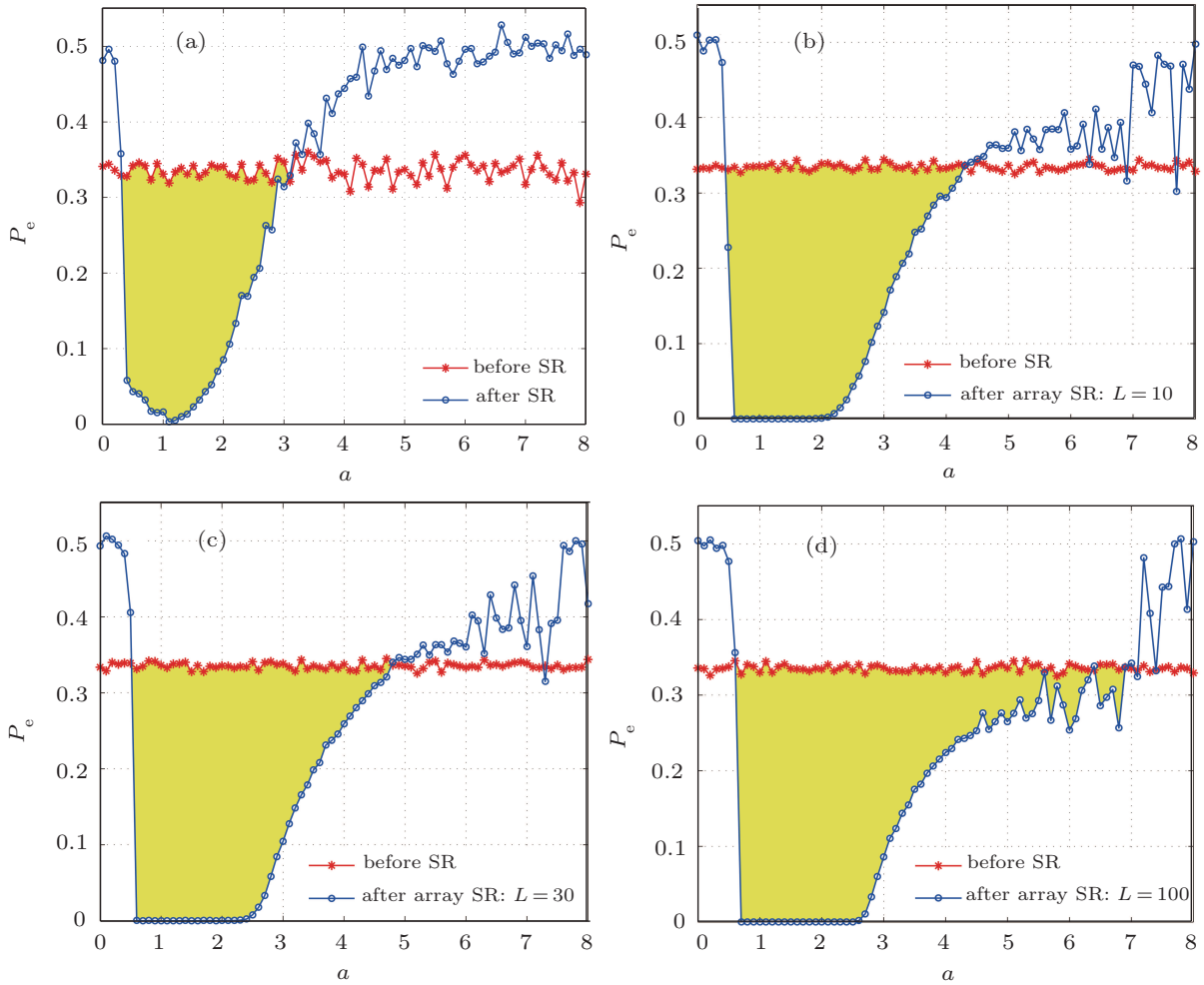


Fig. 3. (color online) The BER of the optimal linear detection and the P-BSR-CS versus parameter a in its default configuration refering to Refs. [19] and [20] (i.e., $A=0.3$, $\sigma_\xi^2=0.5$). (a) Single BSR system. (b) Array BSR system ($L=10$). (c) Array BSR system ($L=30$). (d) Array BSR system ($L=100$).

Herein, we establish the BSR subsystem with optimal parameters $a_{(\mathrm{SR})}^{\mathrm{opt}}$ and $\mu_{(\mathrm{SR})}^{\mathrm{opt}}$ from Eq. (14) and Fig. 3, where the noisy BPAM signal meets the adiabatic approximation condition, as a normalized BSR model.

$$\frac{\mathrm{d}x_j}{\mathrm{d}t} = a_{(\mathrm{SR})}^{\mathrm{opt}} x_j + \mu_{(\mathrm{SR})}^{\mathrm{opt}} x_j^3 + A\sum_{i=1}^{+\infty} S_i G(t - iT_{\mathrm{SR}}) + \sigma_{\xi_{\mathrm{SR}}}\delta(t), \tag{15}$$

where the optimal system parameter $\left(a_{(\mathrm{SR})}^{\mathrm{opt}}, \mu_{(\mathrm{SR})}^{\mathrm{opt}}\right)$ can be searched from the SR-operative region $\left(a_{(\mathrm{SR})}, \mu_{(\mathrm{SR})}\right)$, which is only associated with symbol interval T_{SR} and noise variance $\sigma_{\xi_{\mathrm{SR}}}^2$.

To illustrate the effectiveness of the SR-operative region, in accordance with Ref. [20], we set the amplitude of the BPAM signal $A=0.3$, the symbol interval $T=T_{\mathrm{SR}}=100$,

and the noise variance $\sigma_{\xi}^2 = \sigma_{\xi_{\rm SR}}^2 = 0.5$ satisfying the adiabatic approximation condition, and then the parameter of the BSR subsystems can be selected referring to Eq. (14) and Fig. 3(a). In Fig. 4, we take four pairs of parameter values as $(0.12, 0.0144)$, $(1,1)$, $(1.2, 1.44)$, and $(3,9)$ to demonstrate the importance of parameter selection. It can be seen from Fig. 4, when the parameter is too small (Fig. 4(a)) or too large (Fig. 4(d)), the SR does not work; the appropriate selection of system parameter in Fig. 4(b) $(1,1)$ and Fig. 4(c) (the optimized combination $(1.2, 1.44)$) ensures SR happens, which results in amplifying the signal amplitude (the input BPAM signal amplitude $A = 0.3$ while the output signal amplitude locates in the vicinity of the bistable system stable state $x = \pm\sqrt{a_{\rm (SR)}/\mu_{\rm (SR)}}$).

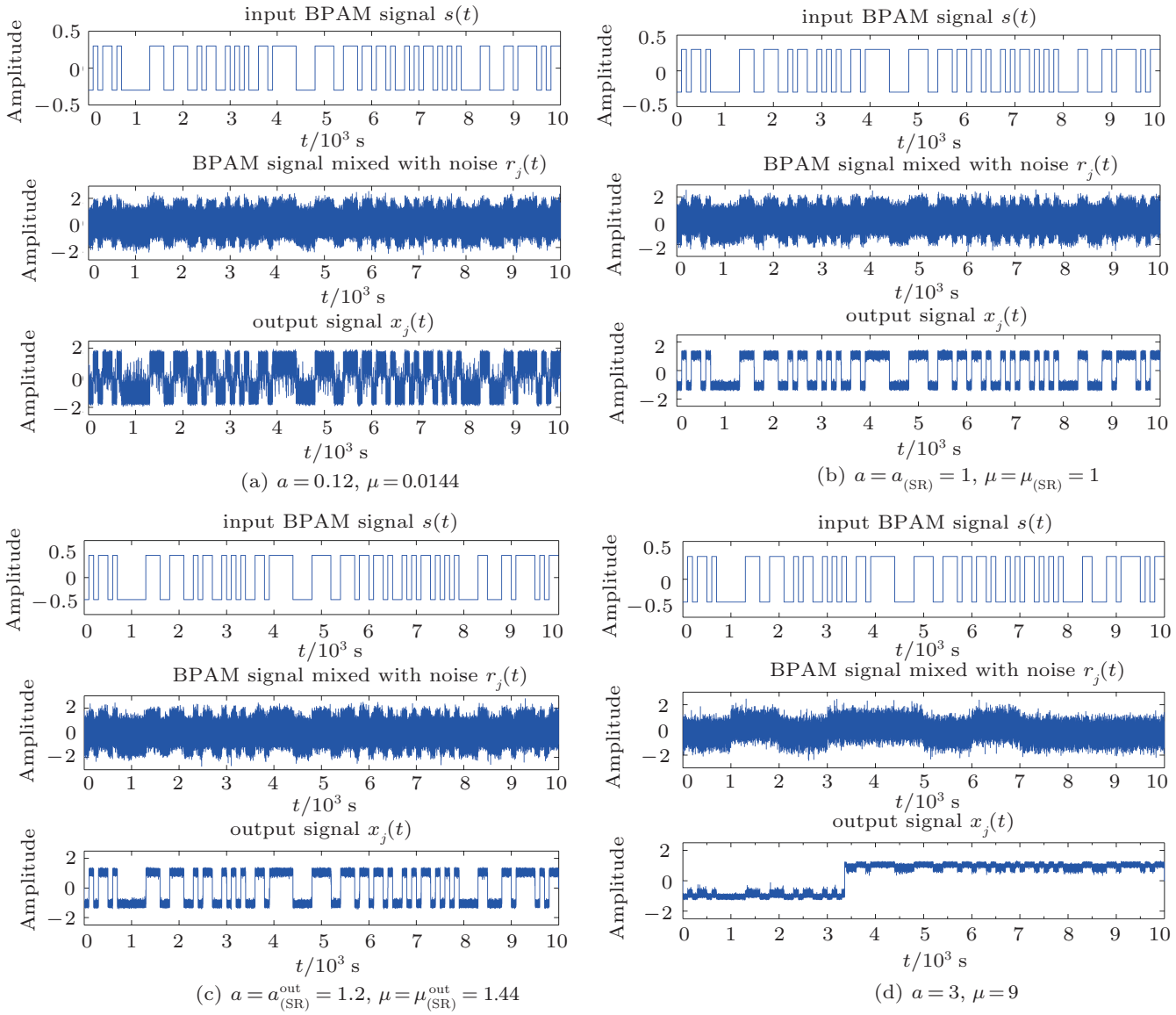


Fig. 4. (color online) Time evolution of the BPAM signal processed by the BSR subsystem (symbol interval $T = T_{\rm SR} = 100$, amplitude $A = 0.3$, and noise variance $\sigma_{\xi}^2 = \sigma_{\xi_{\rm SR}}^2 = 0.5$) for (a) $a = 0.12$, $\mu = 0.0144$; (b) $a = a_{\rm (SR)} = 1$, $\mu = \mu_{\rm (SR)} = 1$; (c) $a = a_{\rm (SR)}^{\rm opt} = 1.2$, $\mu = \mu_{\rm (SR)}^{\rm opt} = 1.44$; (d) $a = 3$, $\mu = 9$.

4. Parameter allocation policy in realistic communication scenarios

In this section, we focus on parameter allocation optimization of the P-BSR-CS for realistic communication scenarios. In Section 3, referring to the adiabatic approximation condition,[16] we have achieved the optimal parameter allocation in the P-BSR-CS that only holds for the input BPAM signal with large symbol interval and the background noise with small variance. However, the idealized assumption of adiabatic approximation does not always exist in practical application circumstances. As a result, to bridge the gap between the aforementioned optimized parameter allocation scheme and practical applications, we intend to resolve the technical feasibility problem of SR for signal transmissions in realistic communication scenarios. By considering the small symbol interval of the BPAM signal ($T \ll 1$) and the large variance of the Gaussian white noise ($\sigma_{\xi}^2 \gg 1$) where the performance amelioration area cannot be reached, we use a variable transfor-

mation to Eq. (6). This principle is to equivalently transform the actual model Eq. (6) to match the normalized BSR model Eq. (15). Therefore, the parameter allocation policy of the P-BSR-CS for maximizing performance in realistic communication scenarios can be obtained in the following steps.

Proposition 1 Consider the realistic communication scenarios, the optimal parameter allocation of the P-BSR-CS is given by

$$\begin{cases} a = a_{(\mathrm{SR})}^{opt}(T_{\mathrm{SR}}/T), \\ \mu = (\sigma_{\xi_{\mathrm{SR}}}^2/\sigma_\xi^2)(T_{\mathrm{SR}}^3/T^3)\mu_{(\mathrm{SR})}^{\mathrm{opt}}, \end{cases} \tag{16}$$

where T and σ_ξ^2 denote the symbol interval of the BPAM signal and the variance of the AWGN in the actual communication, respectively; T_{SR} and $\sigma_{\xi_{\mathrm{SR}}}^2$ denote the pre-setting values in the adiabatic approximation category, $a_{(\mathrm{SR})}^{\mathrm{opt}}$ and $\mu_{(\mathrm{SR})}^{\mathrm{opt}}$ are decided by T_{SR} and $\sigma_{\xi_{\mathrm{SR}}}^2$.

Proof We rewrite Eq. (6) as a general form

$$\frac{\mathrm{d}x_j}{\mathrm{d}t} = ax_j + \mu x_j^3 + s(t) + \xi_j(t), \tag{17}$$

and it constitutes the P-BSR-CS when j varies from 1 to L. Equation (17) can be transformed by using variable transformation as

$$x = \sqrt{\frac{\mu_{(\mathrm{SR})}^{\mathrm{opt}}}{a_{(\mathrm{SR})}^{\mathrm{opt}}}}\sqrt{\frac{\mu}{a}}y, \quad t = \frac{a_{(\mathrm{SR})}^{\mathrm{opt}}}{a}\tau. \tag{18}$$

Substituting Eq. (18) into (17) yields

$$\begin{aligned} \frac{\mathrm{d}y}{\mathrm{d}\tau} &= a_{(\mathrm{SR})}^{\mathrm{opt}}y + \mu_{(\mathrm{SR})}^{\mathrm{opt}}y^3 \\ &+ \sqrt{\frac{(a_{(\mathrm{SR})}^{\mathrm{opt}})^3}{\mu_{(\mathrm{SR})}^{\mathrm{opt}}}}\sqrt{\frac{\mu}{a^3}}A\sum_{i=1}^{+\infty}S_iG(\tau - i\frac{a}{a_{(\mathrm{SR})}^{\mathrm{opt}}}T) \\ &+ \sqrt{\frac{(a_{(\mathrm{SR})}^{\mathrm{opt}})^3}{\mu_{(\mathrm{SR})}^{\mathrm{opt}}}}\sqrt{\frac{\mu}{a^3}}\sigma_{\xi_{\mathrm{SR}}}^2 n(\tau). \end{aligned} \tag{19}$$

By comparing Eq. (19) with Eq. (15), we can gain the parameters a and μ in the case that the input BPAM signal characterized with low symbol interval $(T \ll 1)$ and the noise featured with large variance $(\sigma_\xi^2 \gg 1)$ as $a = a_{(\mathrm{SR})}^{\mathrm{opt}}(T_{\mathrm{SR}}/T)$ and

$$\mu = \left(\sigma_{\xi_{\mathrm{SR}}}^2/\sigma_\xi^2\right)(T_{\mathrm{SR}}^3/T^3)\,\mu_{(\mathrm{SR})}^{\mathrm{opt}}.$$

Hence, we finish the proof of Proposition 1.

At this point, the optimal parameter allocation in the P-BSR-CS can be configured in accordance with Eq. (16), and the implementation steps of performance improvement of the P-BSR-CS are listed below.

Step 1 Under the adiabatic approximation condition $(T \gg 1,\ \sigma_\xi^2 \ll 1)$, a normalized BSR model with optimal parameter searching from the SR-operative region given by Eq. (15) is built to maximize the SR effect.

Step 2 The dynamical equation of bistable system (17) is altered to Eq. (19) based on the variable transformation expression (18), and then the realistic communication scenarios can be mapped to the ideal adiabatic approximation category.

Step 3 From a comparison between Eq. (15) and Eq. (19), an analytical expression of parameter optimization of the P-BSR-CS is derived in Eq. (16).

Step 4 We configure the calculated parameter from Eq. (16) into Eq. (5) and build the optimal parameter allocation policy of the P-BSR-CS to satisfy realistic communication scenarios $(T \ll 1, \sigma_\xi^2 \gg 1)$.

Step 5 By transmitting the noisy signal $r_j(t) = s(t) + \xi_j(t)$ into the corresponding j-th BSR subsystem, we eventually achieve the BER reduction and CC improvement of the P-BSR-CS.

5. Performance analysis

In this section, we will provide theoretical analysis and simulation results to verify the performance improvement brought by the parameter allocation policy of the P-BSR-CS. By using correlation coefficient, the appropriate number of BSR subsystems (array size of the P-BSR structure) is given. Referring to the system model in Fig. 1, the experiment setup is: symbol interval $T = 0.001$, noise variance $\sigma_\xi^2 = 10$. The case $L = 0$ indicates a non-bistable subsystem case.

5.1. Array number of the P-BSR-CS

Based on the central limit theorem (CLT), the P-BSR output $y(t)$ approximately obeys a Gaussian distribution when the array number L is sufficiently large. Generally, the correlation coefficient is used for evaluating how close the degree of nonlinear output response's PDF is to the standard normal distribution function, which leads to the selection number of array L. We define the output response $y(t)$'s PDF as $f_L(y|\mathscr{H}_l)$ $(l = 0, 1)$, the standard normal distribution function as $\varphi(y|\mathscr{H}_l)$. Hence, the similarity of $f_L(y|\mathscr{H}_l)$ and $\varphi(y|\mathscr{H}_l)$ can be denoted by the correlation coefficient, as

$$\rho|\mathscr{H}_l = \frac{L\sum f_L(y|\mathscr{H}_l)\,\varphi(y|\mathscr{H}_l) - \sum f_L(y|\mathscr{H}_l)\sum \varphi(y|\mathscr{H}_l)}{\sqrt{L\sum f_L^2(y|\mathscr{H}_l) - \left(\sum f_L(y|\mathscr{H}_l)\right)^2}\sqrt{L\sum \varphi^2(y|\mathscr{H}_l) - \left(\sum \varphi(y|\mathscr{H}_l)\right)^2}}. \tag{20}$$

In the context of different array size L, the correlation coefficient of the output response $y(t)$'s PDF through P-BSR processing and the standard PDF is shown in Table 1.

Table 1. Correlation coefficient versus the array number.

Correlation coefficient	Array number				
	10	30	50	70	100
$\rho\|\mathscr{H}_l$	0.9936	0.9984	0.9994	0.9997	1.0000

As is seen from Table 1, we note that when the array size of the P-BSR structure is large enough ($L \geq 30$), the correlation coefficient of $f_L(y|\mathscr{H}_l)$ and $\varphi(y|\mathscr{H}_l)$ is very close to 1, which ensures the reliability of using the CLT. However, a larger size of array L is bound to produce more computational complexity and higher design costs. Therefore, we choose an applicable size on the order of 30 ($L = 30$) to pursue the desirable detection performance.

5.2. Comparison analysis of P-BSR case with non-bistable subsystem case

Knowing the AWGN $\xi_j(t)$ submits to a normal distribution, we can conclude that the noisy signal $r_j(t) = s(t) + \xi_j(t)$ also obeys a normal distribution as

$$r_j \sim \begin{cases} \mathscr{N}(A, \sigma_\xi^2), & \text{under } \mathscr{H}_1, \\ \mathscr{N}(-A, \sigma_\xi^2), & \text{under } \mathscr{H}_0. \end{cases} \tag{21}$$

Hence, we can obtain the PDF of the noisy signal $r_j(t)$ as

$$\begin{cases} f(r_j|\mathscr{H}_1) = \dfrac{1}{\sqrt{2\pi\sigma_\xi^2}} \exp\left[-\dfrac{(r_j - A)^2}{2\sigma_\xi^2}\right], \\ f(r_j|\mathscr{H}_0) = \dfrac{1}{\sqrt{2\pi\sigma_\xi^2}} \exp\left[-\dfrac{(r_j + A)^2}{2\sigma_\xi^2}\right]. \end{cases} \tag{22}$$

Denoting the expected value of $x_j(t)$ under hypothesis $\mathscr{H}_1$ and hypothesis $\mathscr{H}_0$ as m_1 and m_0, respectively, and letting the variance of $x_j(t)$ under hypothesis $\mathscr{H}_1$ and hypothesis $\mathscr{H}_0$ as d_1 and d_0, respectively, we have

$$m_1 = E[x_j|\mathscr{H}_1] = \int_{-\infty}^{+\infty} x_j \cdot N_1 \exp\left(-\frac{2U^{(1)}(x_j)}{\sigma_{\xi_j}^2}\right) \mathrm{d}x_j, \tag{23}$$

$$m_0 = E[x_j|\mathscr{H}_0] = \int_{-\infty}^{+\infty} x_j \cdot N_0 \exp\left(-\frac{2U^{(0)}(x_j)}{\sigma_{\xi_j}^2}\right) \mathrm{d}x_j, \tag{24}$$

$$d_1 = D[x_j|\mathscr{H}_1] = \int_{-\infty}^{+\infty} x_j^2 \cdot N_1 \exp\left(-\frac{2U^{(1)}(x_j)}{\sigma_{\xi_j}^2}\right) \mathrm{d}x_j, \tag{25}$$

$$d_0 = D[x_j|\mathscr{H}_0] = \int_{-\infty}^{+\infty} x_j^2 \cdot N_0 \exp\left(-\frac{2U^{(0)}(x_j)}{\sigma_{\xi_j}^2}\right) \mathrm{d}x_j, \tag{26}$$

where

$$\begin{cases} U^{(1)}(x_j) = -ax_j^2\big/2 + \mu x_j^4\big/4 - Ax_j, & \text{under } \mathscr{H}_1, \\ U^{(0)}(x_j) = -ax_j^2\big/2 + \mu x_j^4\big/4 + Ax_j, & \text{under } \mathscr{H}_0, \end{cases} \tag{27}$$

N_1 and N_0 are normalization coefficients for the PDF of $x_j(t)$ under the two hypotheses, respectively, i.e.,

$$N_1 = \left[\int_{-\infty}^{+\infty} x_j \exp\left(-\frac{2U^{(1)}(x_j)}{\sigma_{\xi_j}^2}\right) \mathrm{d}x_j\right]^{-1}$$

and

$$N_0 = \left[\int_{-\infty}^{+\infty} x_j \exp\left(-\frac{2U^{(0)}(x_j)}{\sigma_{\xi_j}^2}\right) \mathrm{d}x_j\right]^{-1}.$$

It follows directly from the CLT that when L is sufficiently large, the output of P-BSR structure y obeys a normal distribution, given as

$$y \sim \begin{cases} \mathscr{N}(m_{y_1}, d_{y_1}) = \mathscr{N}\left(m_1, \dfrac{1}{L}d_1\right), & \text{under } \mathscr{H}_1, \\ \mathscr{N}(m_{y_0}, d_{y_0}) = \mathscr{N}\left(m_0, \dfrac{1}{L}d_0\right), & \text{under } \mathscr{H}_0. \end{cases} \tag{28}$$

Therefore, the PDF of variable y from (28) can be written as

$$\begin{aligned} f(y|\mathscr{H}_1) &= \frac{1}{\sqrt{2\pi d_{y_1}}} \exp\left[-\frac{(y - m_{y_1})^2}{2d_{y_1}}\right] \\ &= \frac{1}{\sqrt{2\pi d_1/L}} \exp\left[-\frac{(y - m_1)^2}{2d_1/L}\right], \end{aligned} \tag{29a}$$

$$\begin{aligned} f(y|\mathscr{H}_0) &= \frac{1}{\sqrt{2\pi d_{y_0}}} \exp\left[-\frac{(y - m_{y_0})^2}{2d_{y_0}}\right] \\ &= \frac{1}{\sqrt{2\pi d_0/L}} \exp\left[-\frac{(y - m_0)^2}{2d_0/L}\right]. \end{aligned} \tag{29b}$$

Now we use $r_{j(c)}$ and y_c to represent the optimal decision threshold of detection in the conventional linear non-bistable case and the P-BSR-CS case, respectively. The optimal decision threshold can be calculated by the maximum likelihood (ML) criterion,[37] yields $r_{j(c)} = y_c = 0$.

According to the maximum a posteriori (MAP) criterion,[37] the BER of the conventional linear non-bistable case and the P-BSR-CS are calculated by

$$\begin{aligned} P_{e(non)} &= P(s(t)|\mathscr{H}_1) \int_{-\infty}^{r_{j(c)}} f(r_j|\mathscr{H}_1) dr_j + P(s(t)|\mathscr{H}_0) \int_{r_{j(c)}}^{+\infty} f(r_j|\mathscr{H}_0) \mathrm{d}r_j \\ &= \frac{1}{2}\left[\int_{-\infty}^{0} f(r_j|\mathscr{H}_1) \mathrm{d}r_j + \int_{0}^{+\infty} f(r_j|\mathscr{H}_0) \mathrm{d}r_j\right] \end{aligned}$$

$$= \frac{1}{2}\left[\int_{-\infty}^{0}\frac{1}{\sqrt{2\pi\sigma_\xi^2}}\exp[-\frac{(r_j-A)^2}{2\sigma_\xi^2}]dr_j+\int_{0}^{+\infty}\frac{1}{\sqrt{2\pi\sigma_\xi^2}}\exp\left[-\frac{(r_j+A)^2}{2\sigma_\xi^2}\right]\mathrm{d}r_j\right], \tag{30}$$

$$P_{\mathrm{e(P-BSR)}} = P(s(t)|\mathscr{H}_1)\int_{-\infty}^{y_c} f(y|\mathscr{H}_1)\,\mathrm{d}y + P(s(t)|\mathscr{H}_0)\int_{y_c}^{+\infty} f(y|\mathscr{H}_0)\,\mathrm{d}y$$

$$= \frac{1}{2}\left[\int_{-\infty}^{0} f(y|\mathscr{H}_1)dy+\int_{0}^{+\infty} f(y|\mathscr{H}_1)\,\mathrm{d}y\right]$$

$$= \frac{1}{2}\left[\int_{-\infty}^{0}\frac{1}{\sqrt{2\pi d_1/L}}\exp\left[-\frac{(y-m_1)^2}{2d_1/L}\right]\mathrm{d}y+\int_{0}^{+\infty}\frac{1}{\sqrt{2\pi d_0/L}}\exp\left[-\frac{(y-m_0)^2}{2d_0/L}\right]\mathrm{d}y\right]. \tag{31}$$

Furthermore, the CC of the conventional linear non-bistable case and the P-BSR-CS can be addressed by using Eqs. (30) and (31), and we have

$$C_{(\mathrm{non})} = \frac{1}{T}[1+P_{\mathrm{e(non)}}\log_2 P_{\mathrm{e(non)}} + (1-P_{\mathrm{e(non)}})\log_2(1-P_{\mathrm{e(non)}})], \tag{32}$$

$$C_{(\mathrm{P-BSR})} = \frac{1}{T}[1+P_{\mathrm{e(P-BSR)}}\log_2 P_{\mathrm{e(P-BSR)}} + (1-P_{\mathrm{e(P-BSR)}})\log_2(1-P_{\mathrm{e(P-BSR)}})]. \tag{33}$$

5.3. Experiment results

In this subsection, we plot the performance curves of BER and CC by theoretical points and simulations. In addition, we discuss the characteristic of BER and CC. The input BPAM signal amplitude is set as $A = 0.3$, the symbol interval $T = 0.001$. Owing to the fixed signal amplitude A, we can achieve the variable input SNR via modulating the input noise variance σ_ξ^2 (SNR $= 10\log_{10}(A^2/\sigma_\xi^2)$). All the simulation results we provided are averaged over 10^7 Monte-Carlo realizations.

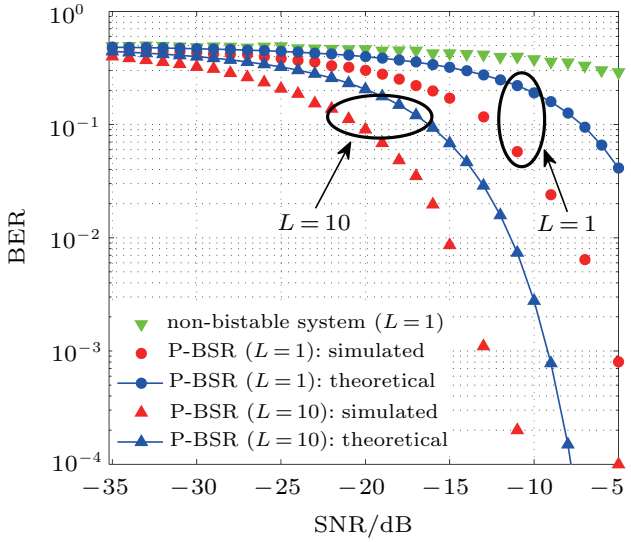


Fig. 5. (color online) BER performance comparison among different array numbers ($L=0$: non-bistable case; $L=1$: single-bistable case; $L=30$: array-bistable case). From top to bottom, the BER is plotted as non-bistable system ($L=0$), P-BSR ($L=1$): simulated, P-BSR ($L=1$): theoretical, P-BSR ($L=10$): simulated, and P-BSR ($L=10$): theoretical.

As seen in Figs. 5 and 6, the BER performances are plotted as functions of input SNR in two detection manners (i.e., the conventional optimal linear case and the P-BSR-CS case). Compared with the conventional optimal linear detection, the novel P-BSR design exhibits a remarkable BER reduction in the case of a weak input BPAM signal. Since we have fixed symbol interval $T = 0.001$, the parameters a and μ can be calculated by Eq. (16) under different noise variance σ_ξ^2. Every SNR value corresponding to an optimal parameter pair $(a^{\mathrm{opt}}, \mu^{\mathrm{opt}})$, which is not optimal for other SNR values. Then, the BER curve is monotonous with the increasing of SNR, which exhibits the classical SR behavior. However, in this paper, we utilize the parameter-induced SR mechanism and the proposed parameter allocation policy to adaptively search the optimal $(a^{\mathrm{opt}}, \mu^{\mathrm{opt}})$ in each SNR value. In practice, the theoretical points and simulations in Figs. 5 and 6 are troughs of these resonance type curves, which devotes to a continuously optimizing resonance effect. The deviation between simulations and theoretical values is attributed to the approximate solution from the Fokker–Planck equation and the use of CLT in the array structure. We also observe that the BER reduction is positively proportional to the size of array L. As the expected value and variance of $x_j(t)$ are obtained, BER is only relevant to the size of array L, which is inversely proportional to the size of array L. Therefore, the BER curves have a decreasing trend in the figures as the size of array L increases, which is the reason that the P-BSR-CS design takes advantage of the array-aided SR effect. The input SNR is set from -35 dB to -5 dB to demonstrate the performance comparison, particularly in low SNR environments. Impressively, the optimal parameter allocation scheme of the P-BSR-CS is of interest to achieve an excellent and reliable performance at low SNR, which satisfies the international communication standard (e.g., IEEE 802.22 with SNR $= -20$ dB).

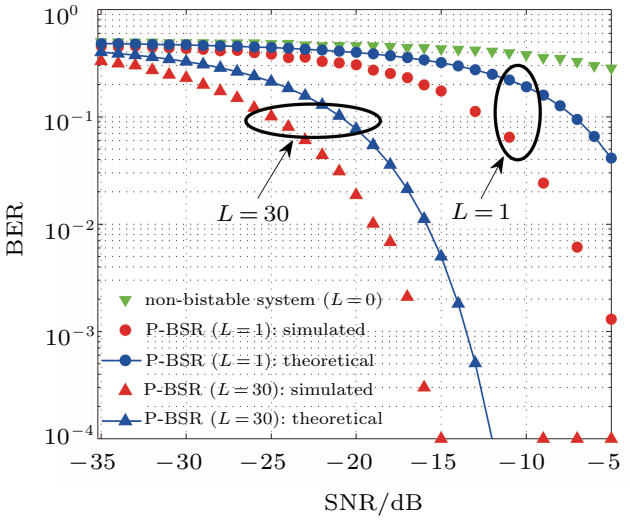


Fig. 6. (color online) BER performance comparison among different array numbers ($L=0$: non-bistable case; $L=1$: single-bistable case; $L=30$: array-bistable case). From top to bottom, the BER is plotted as a non-bistable system ($L=0$), P-BSR ($L=1$): simulated, P-BSR ($L=1$): theoretical, P-BSR ($L=30$): simulated, and P-BSR ($L=30$): theoretical.

In Figs. 5 and 6, only the BER metric is used to demonstrate the reliability of the parameter allocation scheme in the P-BSR-CS. Next, we consider another one, namely CC, to evaluate the efficiency of the P-BSR-CS.

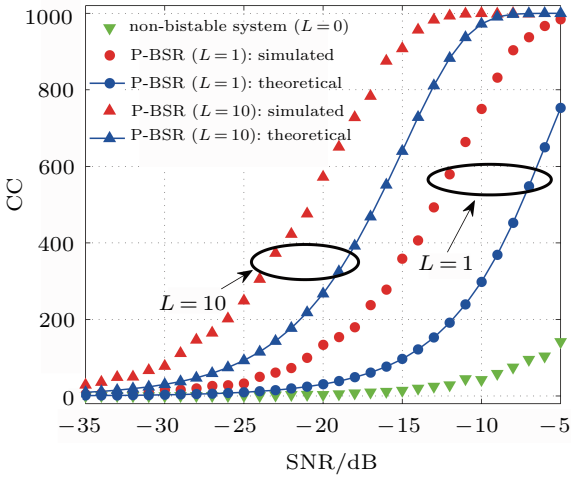


Fig. 7. (color online) CC performance comparison among different array numbers ($L=0$: non-bistable case; $L=1$: single-bistable case; $L=30$: array-bistable case). From bottom to top, the CC is plotted as non-bistable system ($L=0$), P-BSR ($L=1$): simulated, P-BSR ($L=1$): theoretical, P-BSR ($L=10$): simulated, and P-BSR ($L=10$): theoretical.

Figures 7 and 8 compare the CC performance of the P-BSR-CS with that of a conventional optimal linear scenario. It can be seen that the P-BSR-CS based on the proposed parameter allocation scheme is always superior to the conventional one used in signal reception with a much higher CC. The more the size of the array is, the better the CC performance can be achieved. Moreover, the CC improvement is more remarkable in low SNR regimes, for instance, the CC can almost reach the upper bound at -15 dB when $L=30$. This means that, with a restricted performance demand, the P-BSR-CS using the proposed parameter allocation policy can significantly yield a stable and effective performance.

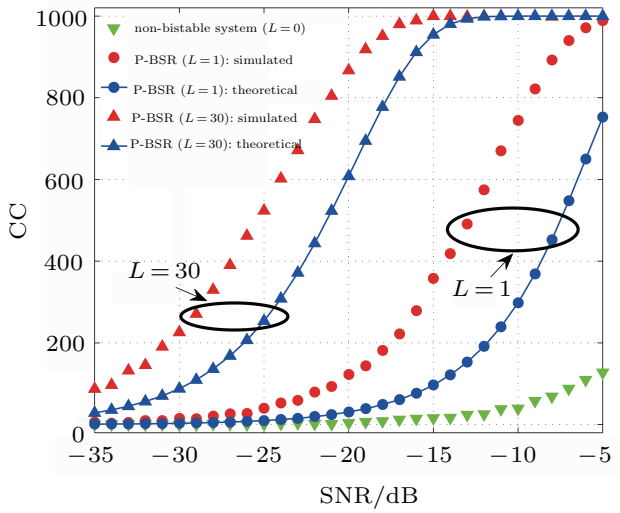


Fig. 8. (color online) CC performance comparison among different array numbers ($L=0$: non-bistable case; $L=1$: single-bistable case; $L=30$: array-bistable case). From bottom to top, the CC is plotted as non-bistable system ($L=0$), P-BSR ($L=1$): simulated, P-BSR ($L=1$): theoretical, P-BSR ($L=30$): simulated, and P-BSR ($L=30$): theoretical.

6. Conclusion

We have proposed a parameter allocation scheme in the P-BSR-CS to meet the requirements for weak BPAM signal transmissions. Under the adiabatic approximation condition, we presented an optimal and robust parameter allocation policy to minimize the BER and maximize the CC of the P-BSR-CS. By considering realistic communication scenarios, a parameter allocation theorem was given for achieving the best SR effect. The optimization problem of parameter allocation in the realistic communication scenario can be mapped into the adiabatic approximation category through variable transformation, which is easy to tackle. Based on the CLT, the semi-closed form expressions of BER and CC were deduced to analyze the P-BSR-CS performance. Our optimal solution has overcome the shortcoming of parameter selection in Refs. [19] and [20], whose strategy lacks the stability and fails to take full advantage of the SR effect. In this paper, the proposed parameter allocation policy can adaptively select the optimal system parameter according to background noise, which yields the best SR effect. Moreover, the design of the P-BSR structure can obtain not only the robustness of optimal parameter selection but also the performance improvement. It is worth noting that a larger array number makes a wider region of parameter selection optimization and higher system performance. However, a larger size of array is bound to produce more computational complexity and higher design costs. Thus, a trade-off between the aforementioned advantages and disadvantages in choosing the array size of the P-BSR structure must be taken into account. Finally, the results demonstrate that the proposed

parameter allocation scheme can achieve much better performance than the existing counterparts in the literature, which contributes significantly to the reliability of signal transmissions in future practical communications.

References

[1] Benzi R, Sutera A and Vulpiani A 1981 *J. Phys.: Math. Gen.* **14** 453
[2] Wang Z Y, Chen P J and Zhang L Y 2015 *Chin. Phys. B* **24** 059801
[3] Guo Y F and Tan J G 2012 *Chin. Phys. B* **21** 120501
[4] Li J H 2014 *Chin. Phys. Lett.* **31** 030502
[5] Uhlich S 2015 *IEEE T. Signal Proces.* **63** 5535
[6] Liu J, Wang Y G and Zhai Q Q 2016 *IEICE T. Fund. Electr.* **99** 323
[7] Kang Y M, Xue J X and Xie Y 2005 *Phys. Rev. E* **72** 021902
[8] Duan F B, Chapeau-Blondeau F and Abbott D 2012 *Signal Process.* **92** 3049
[9] Duan F B, Chapeau-Blondeau F and Abbott D 2011 *Physica A* **390** 2855
[10] Duan F B, Chapeau-Blondeau F and Abbott D 2016 *Phys. Lett. A* **380** 33
[11] McDonnell M D, Stocks N G, Pearce C E M and Abbott D 2008 *Stochastic Resonance: From Suprathreshold Stochastic Resonance to Stochastic Signal Quantization* (Cambridge: Cambridge University Press)
[12] Chen H, Varshney P K, May S K and Michels J H 2007 *IEEE T. Signal Proces.* **55** 3172
[13] Guo G C, Yu X W, Jing Y D and Mandal M 2013 *IEEE Signal Procs. Lett.* **55** 3172
[14] Li Q W and Li Z 2014 *IEEE T. Veh. Technol.* **63** 1717
[15] Xu B H, Duan F B, Bao R H and Li J L 2002 *Chaos, Solitons and Fractals* **13** 633
[16] McNamara B and Wiesenfeld K 1989 *Phys. Rev. A* **39** 4854
[17] Yang D X, Gu F S, Feng G J, Yang Y M and Andrew B 2015 *Chin. Phys. B* **24** 110502
[18] Wang J, Zhang S W, Zhang D M, Li H S and Li S Q 2014 *IEEE T. Wirel. Commun.* **13** 4014
[19] Liu J and Li Z 2015 *IET Commun.* **9** 101
[20] Liu J, Li Z, Guan L and Pan L 2014 *IEEE Commun. Lett.* **18** 427
[21] Stocks N G 2000 *Phys. Rev. Lett.* **84** 2310
[22] Duan F B, Chapeau-Blondeau F and Abbott D 2006 *Electron. Lett.* **42** 1008
[23] Duan F B, Chapeau-Blondeau F and Abbott D 2008 *Phys. Lett. A* **372** 2159
[24] Kang Y M, Jiang J and Xie Y 2012 *J. Stat. Mech.: Theory E.* **10** P10029
[25] Yang J Q, Ma H and Zhong S C 2015 *Acta Phys. Sin.* **64** 170501 (in Chinese)
[26] Qin T Q, Wang F, Yang B and Luo M K 2015 *Acta Phys. Sin.* **64** 120501 (in Chinese)
[27] Tu Z, Lai L and Luo M K 2014 *Acta Phys. Sin.* **63** 120503 (in Chinese)
[28] Lin M, Huang Y M and Fang L M 2008 *Acta Phys. Sin.* **57** 2048 (in Chinese)
[29] Tang Y, Zou W, Lu J Q and Kurths J 2012 *Phys. Rev. E* **85** 046207
[30] Rousseau D, Anand G V and Chapeau-Blondeau F 2006 *Signal Proces.* **86** 3456
[31] Hari V H, Anand G V, Premkumar A B and Madhukumar A S 2012 *Signal Proces.* **92** 1745
[32] Li H and Wang Y G 2014 *Acta Phys. Sin.* **63** 120506 (in Chinese)
[33] Li W, Lu H Z and Zuo Y Y 2014 *Math. Probl. Eng.* **43** 7843
[34] Ma Y M and Duan F B 2014 *Phys. Lett. A* **378** 2651
[35] Zhang X M, Yan J F and Duan F B 2016 *Fluct. Noise Lett.* **15** 1650003
[36] Duan F B and Xu B H 2003 *Int. J. Bifurc. Chaos* **13** 411
[37] Kay S M 2008 *Fundamentals of Statistical Signal Processing, Volume II: Detection Theory*, 3rd edn. (Englewood Cliffs: Prentice-Hall)